Korean J. Chem. Eng., 38(8), 1715-1719 (2021)
DOI: 10.1007/s11814-021-0826-0

pISSN: 0256-1115
eISSN: 1975-7220

Effective pore control and enhanced strength of cellulose acetate using polyethylene glycol for improved battery stability

San Hae Kim*,‡, Yu Ra Choi*,‡, Yoon Jeong Cho*,‡, Seung Yeon Rhyu**, and Sang Wook Kang*,**,†**

*Department of Chemistry and Energy Engineering, Sangmyung University, Seoul 03016, Korea
**Department of Chemistry, Sangmyung University, Seoul 03016, Korea
***Department of Computer Science, Sangmyung University, Seoul 03016, Korea
(*Received 13 November 2020 • Revised 1 February 2021 • Accepted 29 April 2021*)

Abstract−Water-channels were generated into cellulose acetate (CA) via the addition of polyethylene glycol (PEG) and water-assisted pressures. It was found that the PEG used as the plasticizer could enable pores in CA to be controlled. Since the PEG had a relatively small molecular weight, it easily penetrated into polymer chains and formed abundant free volumes in the CA, enabling the pore control. In addition, the PEG enhanced the thermal stability of CA by forming new bipolar interactions and hydrogen bonding between the CA chains and the hydroxyl groups of PEG. From these results, it could be expected that due to the low cost and eco-friendliness of PEG and CA, they could be widely used to manufacture separators used in batteries.

Keywords: Cellulose, Composite, Polyethylene Glycol, Pore, Porosity

INTRODUCTION

With an increase in the growth of the electric vehicle market, the demand for separators, which are major components in secondary batteries, is expected to increase by 40% by the year 2025. According to SNE research, the annual growth rate of the secondary battery separator market in 2020 was 38% [1-3]. The separator, which is one of the four major components of lithium ion batteries [4-7], physically prevents the contact between the positive (cathode) electrode and the negative (anode) electrode [8,9]. This is done by preventing the flow of electrons through the electrolyte and allowing only the passage of desired ions through the fine pores [10-13]. To improve the insulating property of the separator, a microporous polyethylene (PE)-based separator was developed, wherein the size of the pores was adjusted to a micrometer or less [14-17]. Commercially available separators, such as PE- or polypropylene (PP)-based separators, are expensive with low thermal stability and electrochemical performance, and a very important technical issue that affects their stability and battery cycle [18,19].

PE and PP membranes are used extensively as lithium-ion battery separators [20]. However, several factors limit the practical application of these separators. Ying et al. improved the moisture permeability to approximately 396-683 L/m^{2}h using water treatment. The improved moisture permeability was due to the excellent dispersion of BUT-8 (A) and good compatibility between MOF and polymer. To compensate for the low melting point of PP and PE materials, the materials were subjected to a ceramic coating process [21]. However, the high-cost of this method limits its practical application [22].

In this study, to overcome these limitations, cellulose acetate (CA) was used as the separator to enhance the durability and heat resistance of the battery. In addition, to form a straight pore, the pore size and volume of the polymer matrix containing a plasticizer were adjusted using water pressure treatment. The water pressure treatment is an ecofriendly and energy efficient method.

However, due to the poor mechanical strength of CA, it is prone to tearing during the water pressure process. To increase the efficiency of the water treatment method, a plasticizer is added to the polymer to increase the flexibility of the polymer during the water pressure treatment. Plasticizers such as the metal salts of Mg and Ni are usually used to improve the mechanical strength of CA; however, the high cost of these metal salts limits their practical application [23-26]. The poor mechanical strength of CA membrane can be attributed to the weak intermolecular strength of its hydrogen bond. The addition of polyethylene glycol (PEG) to CA can improve the mechanical strength of CA by increasing the intermolecular attraction of its carbonyl group. In this study, PEG, which is highly soluble in solvent (acetone : water=8 : 2) and is unreactive with CA polymer was selected as the plasticizer and expected to be effective for pore-generation. PEG has a high mechanical strength and low-cost synthesis process. In addition, compared to other plasticizers, (DOP, DBP), PEG is environmentally friendly.

The dispersion in the membrane was confirmed by Fourier transform infrared (FT-IR) and thermogravimetric analysis (TGA). Scanning electron microscopy (SEM) and porosimeter were used to confirm the formation of pores after the water pressure treatment.

EXPERIMENT

1. Separator Fabrication

First, a 10% (w/w) solution of CA was obtained by dissolving

†To whom correspondence should be addressed.
E-mail: swkang@smu.ac.kr
‡Equally contributed as first authors.

CA in acetone/water (w/w 8 : 2). To prepare the polymer matrix, the amount of PEG added to the polymer matrix was determined according to the optimal molar ratio of PEG to CA. Then, the final mixture was stirred for two days at room temperature. Subsequently, the resulting solutions were cast on glass plates using a doctor blade to form freestanding films with a thickness of approximately 200 μm, and then the films were dried for 30 min in a thermo-hygrostat at 25 °C and 50% humidity. The dried film containing PEG was then subjected to water pressures ranging from 2 to 8 bar. The water flux of the films with varying porosities was measured and expressed in units of L/m^{2}h (LMH).

2. Characterization

The porosity of the porous CA membrane was examined using the mercury adsorption method (MicroActiveAutoPore V9600, Micromeritics). The pores generated in the polymer were investigated using SEM (JSM-5600LV, JEOL).

FT-IR measurements were carried out on a Varian FTS3100 spectrometer; 64-200 scans were averaged at a resolution of 4 cm^{-1}. TGA was performed with Mettler Toledo TGA devices at a heating rate of 10 °C/min.

RESULTS AND DISCUSSION

1. Porosity of the CA Polymer

To investigate the effect of PEG on the number of pores and the pore size, the water flux of the neat CA and CA : PEG at different water pressure was measured. As reported in previous studies, CA showed low water flux and neat CA shows little change in the water flux even after hydrostatic treatment.

In this experiment, due to the addition of PEG as the plasticizer, water flux was observed in the CA : PEG. To control the pore size in the CA, the CA : PEG was fixed at a ratio of 1 : 0.01, and the water flux of the sample subjected to water pressure from 2 to 8 bar was compared. As shown in Fig. 1, the water flux gradually increased from 30 LMH at 2 bar to 120 LMH at 8 bar. These measurements showed an error range of ±34 values. This result indicates that the water flux constantly increased with an increase in the water pressure, suggesting that the number of formed pores increased with an increase in the water pressure. This confirms the pore control ability of the water pressure treatment, indicating that the pore size can be easily adjusted using this method to suit various application.

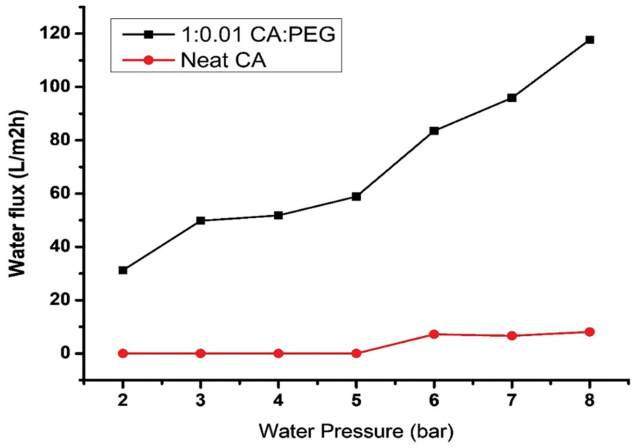

Fig. 1. Measured water flux of the neat CA and 1 : 0.011 CA : PEG from 2 to 8 bar water pressure.

2. Surface Morphology

SEM analysis was used to investigate the effect of PEG on the generation of pores in the CA membrane and the pore control ability of the water pressure treatment. Fig. 2(a) shows the surface morphology of the neat CA without additives and water pressure. As shown in Fig. 2(a), no pores were observed in the neat CA. In contrast, as shown in Fig. 2(b) and (c), pores were observed in the CA : PEG at 5 bar and 8 bar, respectively. The radius of the observed pores in Fig. 2(b) and (c) was 1 μm and 2.5 μm, respectively. These pores were generated homogeneously on the surface of the CA due to the presence of PEG and the application of the water pressure.

The SEM images confirm the generation of pores by the addition of PEG as the plasticizer and the application of water pressure. These results will be useful for controlling the pore size or porosity in the CA membrane. To further understand the pore control ability of the water pressure treatment, the pores in the samples treated at different water pressures were examined. As shown in (Fig. 2(c)) and (Fig. 2(b)), in the SEM image of the sample treated with 8 bar of water pressure, more pores were generated in the CA : PEG at 8 bar compared to the CA : PEG at 5 bar (Fig. 2(b)).

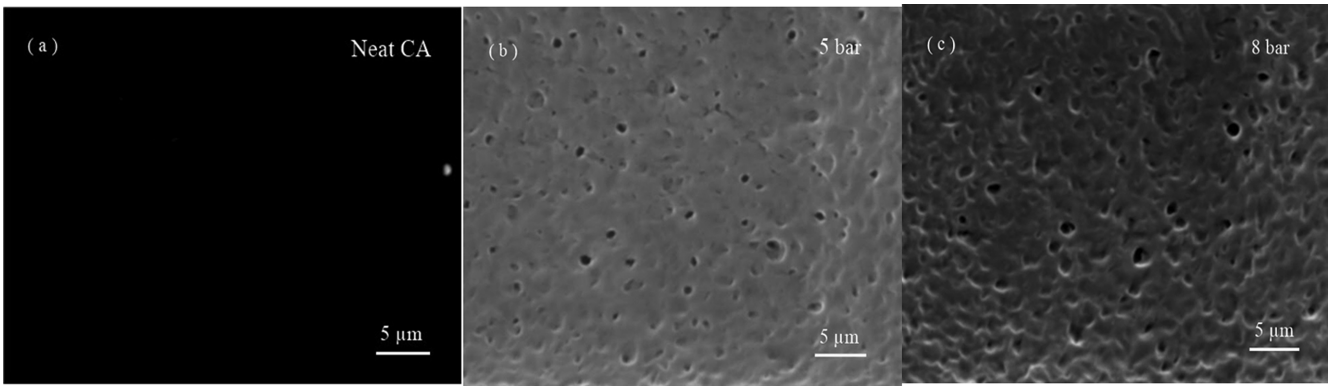

Fig. 2. SEM images: (a) pores observed in the neat CA membrane, (b) pores observed in the CA : PEG at 5 bar, and (c) pores observed in the CA : PEG at 8 bar.

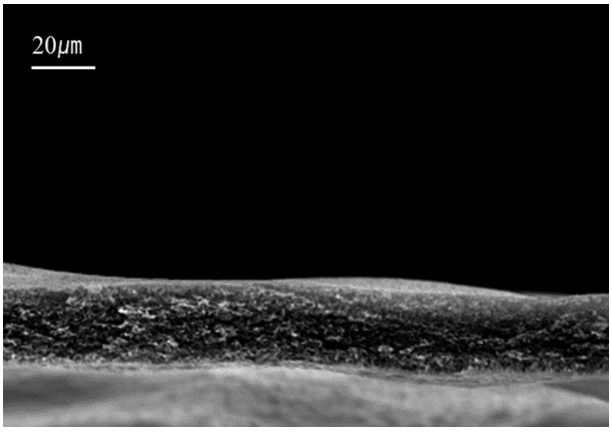

Fig. 3. Cross-sectional image of the CA : PEG at 8 bar.

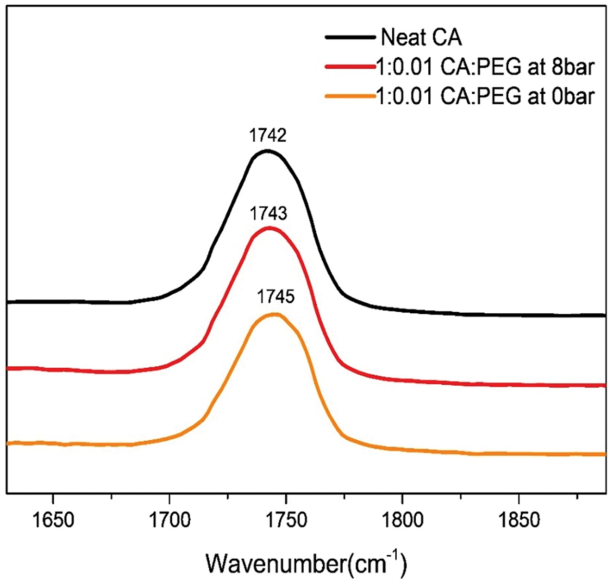

Fig. 4. FT-IR data of the neat CA, 1 : 0.01 CA : PEG at 0 bar, and 1 : 0.01 CA : PEG at 8 bar.

These results indicate that pore size and porosity can be controlled by adjusting the water pressure. This is consistent with the water flux data in Fig. 1. It shows the relationship between the degree of water pressure and pore control.

Cross-sectional SEM images were obtained to investigate the cross-section of the CA : PEG polymer. As shown in Fig. 3, pores were uniformly generated inside the CA : PEG polymer. In addition, the SEM image shows that the pores formed nearly straight lines inside the polymer.

3. Plasticization Effect and Improved Strength of the Polymer

FT-IR data were used to confirm the coordinative interaction of the CA with PEG. The FT-IR spectra of the samples obtained in the range of 1,742-1,745 cm^{-1} in Fig. 4 show the change in the strength of carbonyl bonding. The peak of the neat CA was observed at 1,742 cm^{-1} and that of the 1 : 0.01 CA/PEG (0 bar) was observed at 1,745 cm^{-1}, while the peak at 1,743 cm^{-1} corresponds to the 1 : 0.01 CA/PEG (8 bar).

The peak of the neat CA shifted with the addition of PEG, indicating the weakening of the carbonyl bonding. This is because the hydroxyl group of the PEG formed new interactions in the CA matrix, leading to the weakening of the existing carbonyl bonding. Furthermore, these interactions formed stronger bonds than the existing bonds, thereby increasing the thermal stability of the CA. Neat CA membranes have poor mechanical strength and thermal stability due to the relatively weak interaction between the polymer chains. However, the addition of PEG as a plasticizer to the neat CA induced the formation of new bonds such as the formation of dipolar attraction and new hydrogen bonds. These bonds increased the intermolecular force of the polymer, which led to an improvement in the mechanical strength and thermal stability.

However, the CA related peak of the CA treated with water pressure at 8 bar was higher than that of the neat CA, indicating that the added PEG was not completely removed after water treatment. A more detailed explanation of these phenomena is discussed in the following deconvolution data:

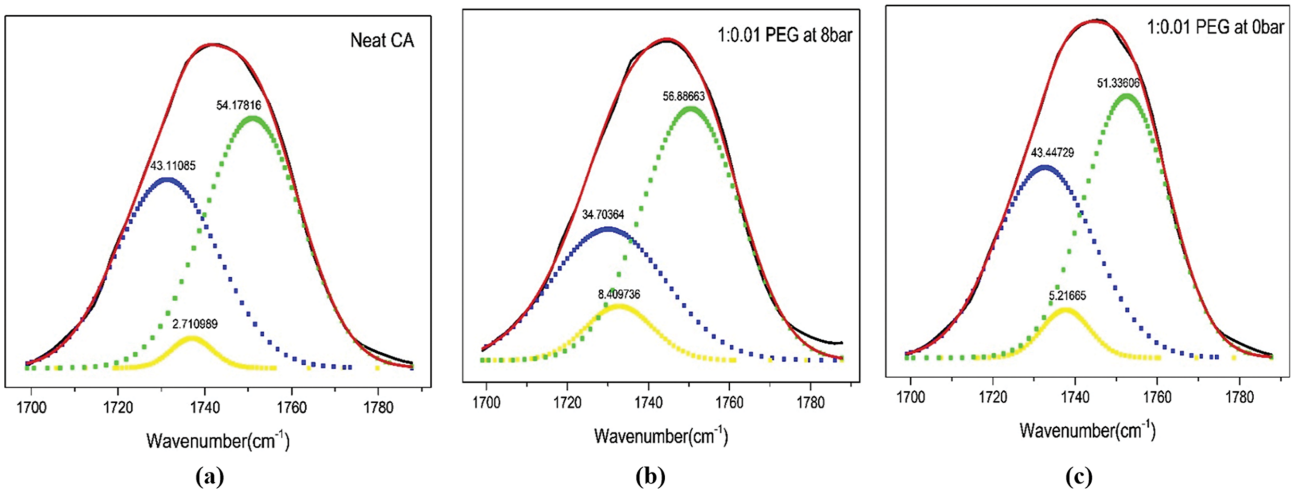

Fig. 5. IR deconvolution data of (a) neat CA, (b) 1 : 0.01 CA : PEG at 0 bar, and (c) 1 : 0.01 CA : PEG at 8 bar.

Table 1. Deconvolution data of (a) neat CA, (b) 1 : 0.01 CA : PEG at 0 bar, and (c) 1 : 0.01 CA : PEG at 8 bar

Peaks	Neat CA	1 : 0.01 CA : PEG at 0 bar	1 : 0.01 CA : PEG at 8 bar
1,731.33 cm^{-1}	43.11%	43.45%	34.70%
1,737.02 cm^{-1}	2.71%	5.22%	8.41%
1,751.04 cm^{-1}	54.18%	51.34%	56.89%

The IR peaks were analyzed by deconvolution, as shown in Fig. 5. Table 1 shows the area ratio of the carbonyl peak of each sample in the 1,732-1,751 cm^{-1} region in Fig. 5. In the neat CA, the peak area at the 1,732-1,735 cm^{-1} region was 43.11%, while the peak area at the 1,732-1,735 cm^{-1} region of CA : PEG at 8 bar was 34.70%, indicating a 9% decrease after water treatment in the presence of a plasticizer. This decrease in peak area can be attributed to the new interaction generated by PEG, indicating that the carbonyl group peak was weakened. Due to the strength of the new bond, the PEG was retained in the CA even after the water treatment.

Since PEG existed in the CA matrix, solvation by the solvent molecules became easier and the polymer became more flexible. As shown in Fig. 6, since the PEG had a relatively small molecular weight (MW 400) and high mobility, it could form a flexible region in polymer matrix according to the free volume theory, thus increasing the plasticization effect in the PEG. The flexibility of the CA polymer increased because it formed strong interactions with the solvent molecules (water and acetone). Consequently, the increase in the flexibility of the polymer facilitated the formation of pores during the water pressure treatment.

4. Thermal Stability

TGA was performed to examine the thermal stability of the porous polymer matrix using a Universal V4.5 A (TA Instruments). Fig. 7 shows that the neat CA, CA : PEG at 0 bar, and the CA : PEG at 8 bar decomposed at a temperature of approximately 320 °C. Specifically, Fig. 8 shows the decomposition difference for neat CA, CA : PEG at 0 bar, and the CA : PEG at 8 bar. The neat CA shows approximately 3% more weight loss than the CA : PEG at 0 bar. This can be attributed to the new interaction generated when PEG was added, which in turn strengthened the neat CA chains.

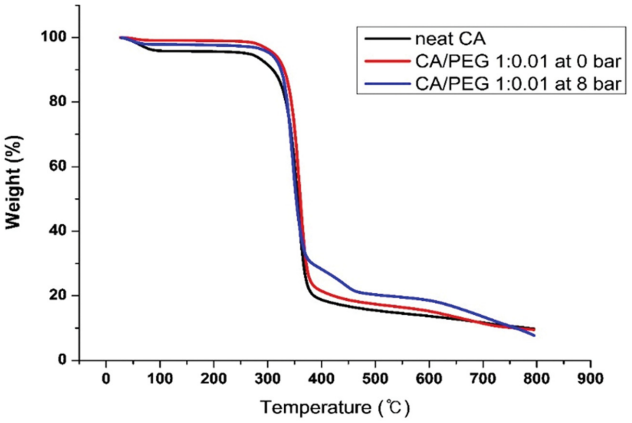

Fig. 7. TGA data of the neat CA, 1 : 0.01 CA : PEG at 0 bar, and 1 : 0.01 CA : PEG at 8 bar.

Additionally, at 200 °C before decomposition, the neat CA and CA : PEG at 8 bar showed a 2% weight loss difference. Furthermore, at 400 °C, there was a 10% difference in weight loss due to the retained PEG in the CA even after the water treatment. This increase in thermal stability indicates that the retained PEG molecules formed strong bonds in the CA membrane, which is consistent with the IR analysis. We believe that the increase in the thermal stability of the CA : PEG after water treatment at 8 bar was due to the removal of some of the PEG content by water treatment.

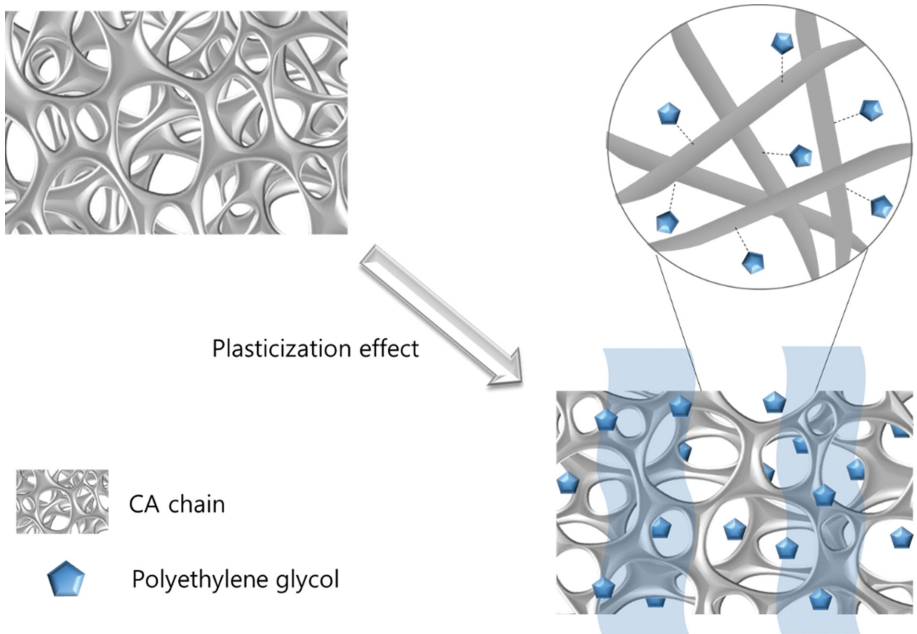

Fig. 6. Scheme of the plasticizing effect by PEG in CA.

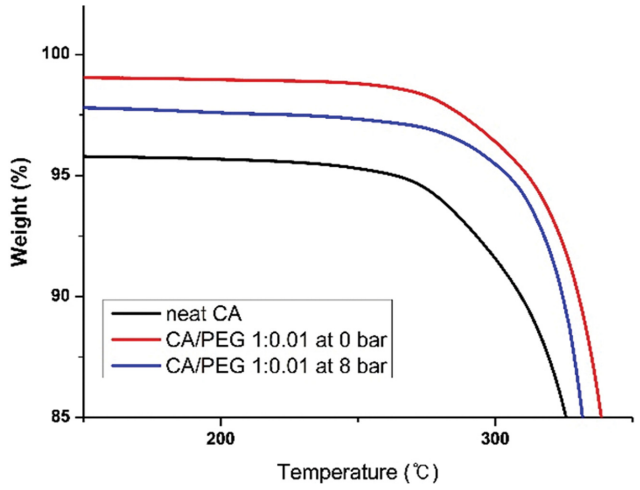

Fig. 8. TGA data: the enlarged area of Fig. 7.

CONCLUSION

PEG was added as a plasticizer to CA polymer, after which water pressure treatment was performed to enable the generation of pores in the CA matrix. It was found that the PEG addition and water pressure treatment had pore control abilities, thereby affecting the generation of pores. In addition, it was observed that the PEG was retained in the CA membrane after water pressure treatment at 8 bar, thus reinforcing the mechanical strength and thermal stability of the CA by forming new dipolar interactions and hydrogen bonding between the CA chains and the hydroxyl group of PEG. The high thermal stability and abundant pores of the CA : PEG after water pressure treatment indicates that the CA : PEG can be utilized in various industrial applications, especially in battery separators and water-treatment membranes used in microfiltration.

ACKNOWLEDGEMENTS

This work was supported by the Basic Science Research Program (2020R1F1A1048176) through the National Research Foundation of Korea (NRF), funded by the Ministry of Science, ICT, and Future Planning.

REFERENCES

1. E. Lizundia, C. M. Costa, R. Alves and S. L. Ménedez, *Carbohydr. Polym. Technol. Appl.*, **1**, 100001 (2020).
2. S. Ou, Z. Lin, X. He, S. Przesmitzki and J. Bouchard, *Trans. Res. Part D*, **81**, 102248 (2020).
3. T. Dong, W. U. Arifeen, J. Choi, K. Yoo and T. Ko, *Chem. Eng. J.*, **398**, 125646 (2020).
4. X. Han, L. Lu, Y. Zheng, X. Feng, Z. Li, J. Li and M. Ouyang, *eTransportation*, **1**, 100005 (2019).
5. C. Zhu, J. Zhang, J. Xu, X. Yin, J. Wu, S. Chen, Z. Zhu, L. Wang and H. Wang, *Carbohydr. Polym.*, **248**, 116753 (2020).
6. X. Huang, *J. Power Sources*, **323**, 17 (2016).
7. W. U. Arifeen, M. C. Kim, D. Ting, R. Kurniawan, J. W. Choi, K. W. Yoo and T. J. Ko, *Mater. Chem. Phys.*, **245**, 122780 (2020).
8. X. Liang, Y. Yang, X. Jin and J. Cheng, *J. Mater. Sci. Technol.*, **32**(3), 200 (2016).
9. Y. Shao, S. Xu, X. Zhao, J. Lim Z. Hu, C. Fang, J. Hu, D. Guo and M. Ouyang, *Int. J. Hydrogen Energy*, **45**, 3108 (2020).
10. C. S. Lee, J. H. Lee, M. S. Park and J. H. Kim, *Korean Chem. Eng. Res.*, **57**, 392 (2019).
11. L. Miao, H. Huan, Z. Wang, Y. Lv, W. Xiong, D. Zhu, L. Gan and L. Li, *Chem. Eng.*, **382**, 122945 (2020).
12. E. Bakangura, C. Cheng, L. Wu, X. Ge, J. Ran, M. I. Khan, E. Kamana, N. Afsar, M. Irfan, A. Shehzad and T. Xu, *J. Membr. Sci.*, **537**, 32 (2017).
13. J. Wang, Y. Xia, Y. Liu, W. Li and D. Zhao, *Energy Storage Mater.*, **22**, 147 (2019).
14. W. Xu, Z. Wang, L. Shi, Y. Ma, S. Yuan, L. Sun, Y. Zhao, M. Zhang and J. Zhu, *ACS Appl. Mater. Interfaces*, **7**, 20678 (2015).
15. Y. M. Lee, N. S. Choi, J. A. Lee, W. H. Seol, K. Y. Cho, H. Y. Jung, J. W. Kim and J. K. Park, *J. Power Sources*, **146**, 431 (2005).
16. Y. M. Lee, J. W. Kim, N. S. Choi, J. A. Lee, W. H. Seol and J. K. Park, *J. Power Sources*, **139**, 235 (2005).
17. L. Sheng, R. Xu, H. Zhang, Y. Bai, S. Song, G. Liu, T. Wang, X. Huang and J. He, *J. Electroanal. Chem.*, **873**, 114391 (2020).
18. P. Lyu, X. Liu, J. Qu, J. Zhao, Y. Huo, Z. Qu and Z. Rao, *Energy Storage Mater.*, **31**, 195 (2020).
19. B. Liu, Y. Jia, C. Yuan, L. Wang, X. Gao, S. Yin and J. Xu, *Energy Storage Mater.*, **24**, 85 (2020).
20. W. G. Lee, D. H. Kim, W. C. Jeon, S. K. Kwak, S. J. Kang and S. W. Kang, *Sci. Rep.*, **7**(1), 1287 (2017).
21. Y. Meng, L. Shu, L. Liu, Y. Wu, L. H. Xie, M. J. Zhao and J. R. Li, *J. Membr. Sci.*, **591**, 117360 (2019).
22. W. Qiu, C. An, Y. Yan, J. Xu, Z. Zhang, W. Guo, Z. Wang, Z. Zheng, Z. Wang, Q. Deng and J. Li, *J. Power Sources*, **423**, 98 (2019).
23. J. M. Li, C. S. Hu, J. M. Shao, H. J. Li, P. Y. Li, X. C. Li and W. D. He, *Polymer*, **119**, 152 (2017).
24. H. Y Kim, Y. Cho and S. W. Kang, *J. Ind. Eng. Chem.*, **78**, 421 (2019).
25. W. G. Lee and S. W. Kang, *J. Ind. Eng. Chem.*, **70**, 103 (2019).
26. J. H. Hwnag, J. S. Choi, J. M. Kim and S. W. Kang, *Macromol. Res.*, **24**, 1020 (2016).